sustainability

MDPI

Article

Structural Performance Assessment of Geothermal Asphalt Pavements: A Comparative Experimental Study

Mohamed Ezzat Al-Atroush [1,*], Abdulrahman Marouf [2], Mansour Aloufi [2], Mohamed Marouf [2], Tamer A. Sebaey [1,3] and Yasser E. Ibrahim [1]

[1] Department of Engineering Management, College of Engineering, Prince Sultan University, Riyadh 11543, Saudi Arabia
[2] Structures and Materials (S&M) Research Laboratory, Prince Sultan University, Riyadh 11543, Saudi Arabia
[3] Mechanical Design and Production Department, Faculty of Engineering, Zagazig University, Zagazig 44519, Egypt
* Correspondence: mezzat@psu.edu.sa; Tel.: +966-5-0636-2379

Abstract: This paper introduces shallow geothermal systems as a potential solution for improving the thermo-mechanical performance of asphalt under extreme climate events. With the recent changes experienced in the climate, earlier infrastructure failure can be expected, predominantly for temperature-sensitive flexible pavements. With that in mind, the efficiency of geothermal systems in terms of heating and cooling was comprehensively argued in many studies. However, very limited studies discussed the structural performance of geothermal pavements. This study conducted a comparative experimental study to assess the change in the compressive and flexural strengths of asphalt under extreme heating and cooling conditions and to evaluate the change in asphalt structural performance due to integrating different types of geothermal pipes into the asphalt structure. This comparative analysis employed thirty-three asphalt specimens with and without copper and polyvinyl chloride (PVC) geothermal pipes. The results of this study show that the geothermal pipes negatively affected the compressive strength of the asphalt at a normal average temperature. However, their effect was relatively minimal on the asphalt (AC) compressive strength under extreme heating and cooling conditions. In contrast, under three thermal conditions—normal, heating, and cooling temperatures—the flexure strength of the AC was significantly improved by 14.3%, 85%, and 70%, respectively, due to the copper pipe integration into the AC. The study concluded that copper pipes were superior to PVC ones in terms of enhancing the AC structural performance.

Keywords: climate change; asphalt pavement; geothermal systems; copper and polyvinyl chloride; comparative experimental study

Citation: Al-Atroush, M.E.; Marouf, A.; Aloufi, M.; Marouf, M.; Sebaey, T.A.; Ibrahim, Y.E. Structural Performance Assessment of Geothermal Asphalt Pavements: A Comparative Experimental Study. *Sustainability* **2022**, *14*, 12855. https://doi.org/10.3390/su141912855

Academic Editors: Qingli (Barbara) Dai, Jie Ji, Songtao Lv, Tao Ma, Dawei Wang and Hui Yao

Received: 9 September 2022
Accepted: 7 October 2022
Published: 9 October 2022

1. Introduction

The United Nations [1] defines climate change as long-term shifts in temperatures and weather patterns, whether these shifts are natural due to solar cycle variations or unnatural due to human activities such as burning fossil fuels, oil, and gas. With that in mind, the ocean and average global land surface temperature reported in March 2020 was 1.16 °C (2.09 °F) higher than the 20th century average of 12.7 °C (54.9 °F), representing the second hottest record in the last 141 years [2]. With this recent rapid change in the climate, earlier infrastructure failure and an increase in maintenance costs can be expected, predominantly for flexible pavements where temperature is an essential driver in selecting construction materials.

On the flip side, asphalt pavements contribute to global warming; several studies addressed that asphalt releases up to 300% more emissions when subjected to solar radiation (i.e., [3,4]). The high covering percentage of the built environment with asphalt pavements may represent a severe hazard concerning the quality of air, especially during the sunny, hot summertime [5]. For instance, 94% of paved roads in the United States are asphalt

pavements [6]. Ultimately, the negative environmental changes may cause faster pavement deterioration, and vice versa; the pavements harm the climate and significantly contribute to global warming.

The structural design of the roadways has to satisfy three fundamental requirements: safety, serviceability, and longevity [7–9]. The current roadway design standards rely on climate data from 1964 to 1995 for pavement material selection [10]. Thus, the material selection for highway construction is often based on the assumption of a stationary climate. Underwood et al. [10] reported that these stationary climate assumptions led to the inappropriate selection of 35% of the pavement materials utilized in 799 different observed locations. This has resulted in different pavement failures and distresses, as reported in a recent assessment study conducted by Transportation for America [11] to evaluate the condition of the roadways across the United States between 2009 and 2017. This study concluded that the percentage of roadways in a poor condition increased from 14 to 20%. As a result, about USD 231.4 billion per year is required to maintain and repair the nation's roads over a six-year period.

In the same vein, asphalt mixture can be described as a temperature-sensitive material [12,13]. Asphalt mixture is composed of an aggregate and a binder, and its performance is likely to vary depending on the temperature variables. The binder stiffness decreases when the temperature increases. That is why pavement distresses, such as reflective and fatigue cracking and many others, are directly and indirectly associated with the temperature state of the asphalt mixture. Several studies [14–16] conducted atomic force microscopy (AFM) to study the effect of thermal aging on the microstructure and components of asphalt mixture. The AFM analysis showed that asphalt pavement has different microstructures upon the change in thermal aging times, and there were significant differences in the nano size of the typical microstructure [17].

Several studies have proven the efficiency of environmentally friendly shallow geothermal systems in controlling the thermal performance of asphalt structures [18,19]. In many cases, through the heat exchange with the underlying subgrade layers, ground source heat pumps (GSHP) can successfully cool down asphalt pavements during the hot summertime and warm them up to be used for ice melting during the cold wintertime [20]. Other studies have also highlighted how this positively contributed to lowering the induced emissions and latent heat from asphalt pavements, enhancing the surrounding atmosphere temperature, and mitigating the urban heat island effects [21].

A geothermal pavement basically comprises the horizontal heat exchanger GSHP system in the conventional pavement layers. As shown in Figure 1, a geothermal pavement consists of three main components. The primary unit consists of heat exchanging loops installed in the pavement layer. The secondary unit comprises the underground pipe network, also known as geothermal pipes (GEP), that delivers the heat energy to or from the subgrade layer. Lastly, the heat pump system is responsible for the continuous movement of the carrier fluid [20,22].

The primary unit consists of a closed-circuit network of pipes embedded in the pavement layer. It collects the heat extracted from the pavement and transfers it to the ground. Those loops can be installed in bridge decks, roads, and airport runways for de-icing purposes [23,24]. The pipes that convey the heat carrier fluid are known as geothermal pipes (GEP), heat transfer pipes, energy loops, or absorber pipes. The geothermal pipes are usually made from high density polyethylene/polypropylene (HDPE/HDPP), polyvinyl chloride (PVC), and polybutylene [25–28]. In addition, several studies reported that using copper material in the pipe network achieves the most outstanding efficiency of the system in terms of heat collection from the asphalt and heat exchange with the soil (e.g., [29]). It is fundamental to mention that most of the previous studies only focused on assessing the thermal behavior of different pipe materials and their efficiency in the heat exchange process, regardless of their influence on the structural performance of the asphalt.

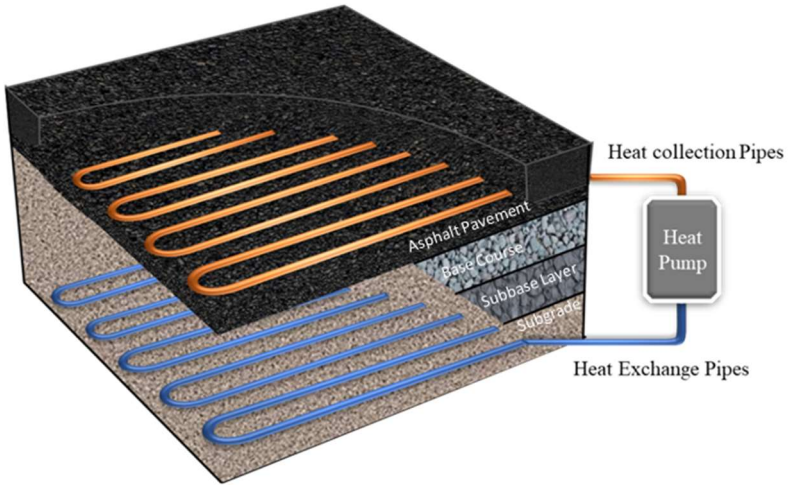

Figure 1. Schematic representation of a geothermal pavement system.

Numerous studies have evidenced the remarkable merits of geothermal systems in improving the thermal performance of asphalt pavements under different climate conditions. However, very few studies have investigated the impact of geothermal systems on the structural performance of asphalt pavements. Practically, either positive or negative impacts could be expected. A positive enhancement in the structural performance of asphalt could be anticipated due to its expected temperature adaptation through the heat exchange with the subgrade. In contrast, the volume loss in the asphalt body due to inserting the geothermal pipes may negatively affect the compressive and flexural performance of the asphalt structure.

This paper aspires to discuss the performance of the asphalt pavement structure under extreme climate conditions. It also introduces a shallow geothermal system as a potential solution for improving the thermo-mechanical behavior of asphalt pavements. An experimental study is carried out to assess the change in the compressive and flexural strengths of asphalt under extreme heating and cooling conditions. A comparative analysis is also performed to evaluate the change in the asphalt structural performance due to integrating different types of geothermal pipes into the asphalt structure. The findings of this study may be beneficial in renovating the current structural design methods of roadways to take into consideration the effect of extreme climate events rather than relying on a stationary climate condition.

2. Materials and Methods

The structural performance of asphalt pavements is investigated in this study by simulating a real-life case of a major roadway located in Riyadh, Saudi Arabia. This study zone has been selected to represent extreme climate conditions. The asphalt pavement temperature was recorded at the mid-thickness of the asphalt layer during the twelve months of the year. It was found that the average monthly temperatures of the asphalt during the hot and cold climates were 60 °C and 2 °C, respectively.

In the same vein, this experimental study also adopted the exact proportions of the hot mix asphalt (HMA) utilized in paving the mentioned roadway case. The Saudi Ministry of Municipal and Rural Affairs developed the general specifications for urban roads [30] to unify the technical rules and standards of roadway construction works. The Saudi standards provide six classes of hot asphalt mixes (A–D); they are classified based on the different roadway classes. Hot mix asphalt type (A) should be utilized for major roadways as the Saudi standards recommend, and it was also the same HMA type utilized in paving the roadway case considered in this study.

The materials used for preparing the laboratory HMA (type A) included; coarse aggregates of crushed stone with uniform consistency, fine aggregates of dense sand, and

bitumen as a binder material. The coarse aggregates and fine aggregates were locally available in the market. The dry sieving was carried out following ASTM D6913-04 [31]. Thus, the particle size distribution curve of the aggregates was obtained, as shown in Figure 2. Furthermore, the 60/70 grade of bitumen was employed in this study. The physicochemical properties were evaluated using standard apparatus according to AASHTO specifications [32], as summarized in Table 1. The Marshall stability method was employed for the hot asphalt mix design. The prepared mixture was examined to ensure that it fulfilled the Saudi standards for HMA type A (Table 2).

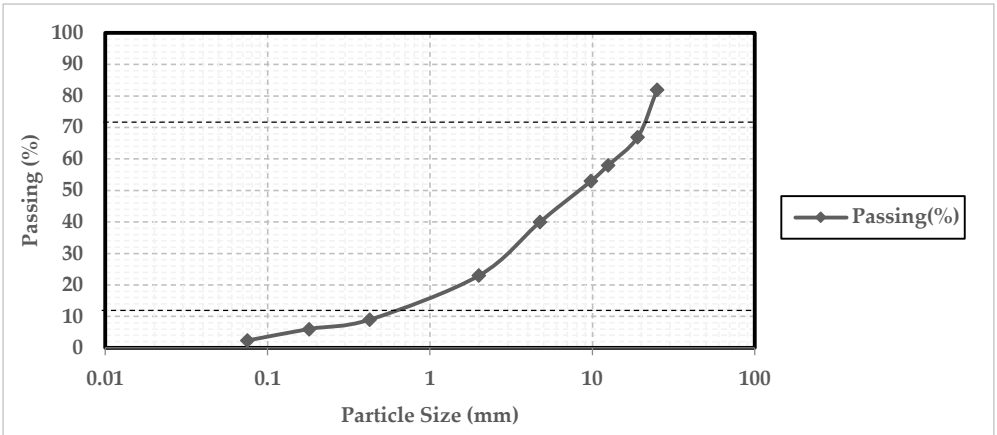

Figure 2. Grain size distribution of the utilized aggregates in asphalt mixtures.

Table 1. Physicochemical properties of bitumen.

Type of Test	Test Method	Units	Results	Specification
Penetration @25 °C	ASTM D5-97	0.1 mm	66	60–70
Softening Point	ASTM D36	1 °C	55	40–55
Flash Point	ASTM D92-16b	1 °C	302	232 min
Ductility 25 °C	ASTM D113	cm	99	Greater than 75

Table 2. Asphalt mix properties.

The Adapted Properties of the Asphalt Mix (Type A) [30]	
Properties	**Boundaries**
Bitumen Percentage from Whole Mixture (%)	4.25
Average Stability (Minimum) (N)	1000
Average Flow (mm)	3.0
Air Void Percentage for Mixture (%)	4.0
Percentage of Voids Filled with Asphalt (%)	70
Voids in Mineral Aggregate (%)	13
The Total Specific Gravity of the Aggregate Mixture	2594.000

On the other hand, this study also aspires to assess the change in the structural performance of asphalt pavements due to the integration of geothermal pipes into the asphalt structure. Therefore, two types of geothermal pipes were utilized with the asphalt pavement. First was the seamless copper pipes. According to ASTM B-280 [33], the copper C10200 type was selected due to its high thermal conductivity that fits the heat exchange application. The second pipe type was made of polyvinyl chloride (PVC). The two pipe types used in this study were 5/8′ (15.8 mm) in diameter. Table 3 compares the mechanical and thermal properties of the two geothermal pipes.

Table 3. Mechanical and thermal properties of the utilized geothermal pipes.

Pipe Material	Copper [34]	Polyvinyl Chloride [35]
Ultimate Tensile Strength	220.6 MPa	51.71 MPa
Modulus of Elasticity in Tension	117.2 GPa	2.83 GPa
Melting Point	1082.8 °C	177 °C
Thermal Conductivity	391 W/mK	0.16 W/mK
Thermal Expansion Coefficient	16.16 µm/mK	5×10^{-5} mm/(mm °C)
Density	8.94 gm/cu cm at 20 °C	1.41 gm/cm^3
Specific Heat Capacity	385.48 J/kg °C	1000 J/(kg.K)

2.1. Methodology of the Experimental Study

The structural performance of both the conventional and geothermal pavement has been investigated through experimental tests, including the Marshall stability test [36], axial compression test [37], and flexural three-point bending test [38]. The three tests were performed under three thermal conditions: the average room temperature (20 °C), the heating condition (60 °C), and the cooling condition (2 °C). This comparative analysis was carried out by testing thirty-three asphalt specimens without and with geothermal pipes, either copper or PVC pipes.

The prepared specimens were divided into three groups; each group consisted of nine specimens. In each group, three specimens were conventional asphalt concrete (AC), three specimens with copper pipes (5/8′ in diameter), and three with PVC pipes with a diameter of 5/8′ in. Moreover, six specimens were prepared to ensure the consistency of the asphalt mixture throughout the whole experiment. Three of them were tested under compression to examine the effect of mixture density, and the other three were tested in Marshall tester to ensure the characteristics of the asphalt mixture.

2.2. Samples Preparation

Cylindrical specimens of 100 mm diameter were prepared for the Marshall test, and 100 mm cubic specimens were used for the compression test; in addition, as shown in Figure 3, the dimensions of the specimens adopted for the flexure test were 100 mm × 500 mm × 100 mm.

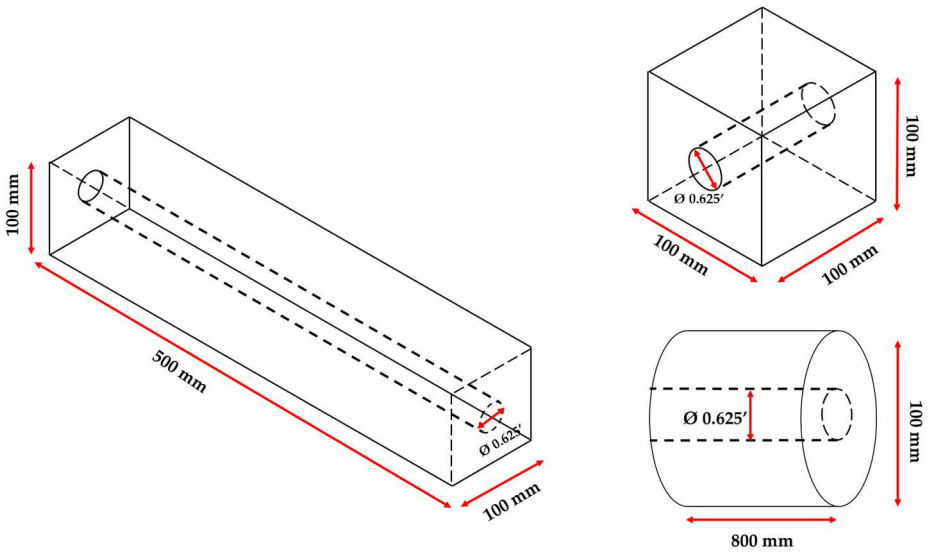

Figure 3. The geometry of the three types of samples employed in the comparative experimental study.

For each specimen, the necessary amount of the dry blended aggregates was calculated to satisfy the consistency requirements of the specimen density. The blended aggregates were heated to 160 °C. The heated aggregate was placed in a pan and thoroughly mixed. A

crater was formed in the aggregate, and the 60/70 penetration grade bitumen was added after it was heated to 160 °C. The aggregates and the bitumen were thoroughly mixed until the aggregates were well coated. The thoroughly cleaned specimen mold assembly and the compaction hammer were heated to 160 °C. The temperature of the mixture immediately prior to compaction was maintained at 150 °C. On average, fifty blows on each face were sufficient for the compaction of the specimens.

After compaction, the base plate was removed, and the mold containing the specimen was immersed in cool water for 2 min. Then, the specimen was removed from the mold employing a sample extractor and a suitable jack and frame arrangement. The specimen was placed on a smooth, flat surface and allowed to cool at room temperature. The specimens were weighed in air and clean water at room temperature. The difference between these two weights was used to determine the volume of the specimens without pipes [39,40]. Thus, the density was obtained.

For the specimens with pipes, the interface between the asphalt material and geothermal pipes is one of the significant concerns that may influence the structural capacity of a geothermal pavement. Therefore, the compaction quality of the asphalt material around the geothermal pipes was a fundamental task that received essential attention during the preparation of the specimens. Polyvinyl chloride and copper were the materials utilized in the experimental study. The pipes were adjusted at the centerlines of the asphalt specimens. In addition, the volume loss due to pipe integration was considered when determining the density of these specimens. Table 4 summarizes the properties of the thirty-three specimens. In addition, Figure 4 shows the first group of the prepared samples (9 specimens per group).

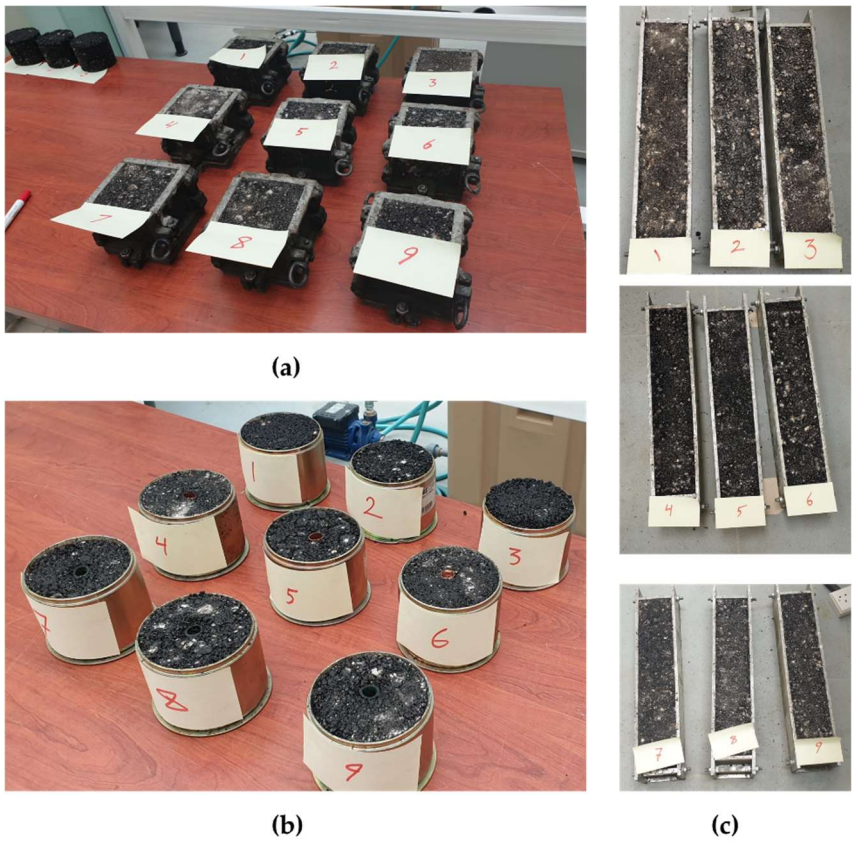

Figure 4. The first group of the prepared specimens for testing at average room temperature. (**a**) Compression test's specimens. (**b**) Marshall stability test's specimens. (**c**) Flexure test's specimens.

Table 4. The characteristics of the prepared thirty-three specimens.

No.	Specimen ID	Geothermal Pipe Material	Dimension (mm)			Density (gm/cm^3)	Test Performed	Thermal Condition (°C)
			Width/Diameter (mm)	Length (mm)	Height (mm)			
1	AC-C1	-	100	100	100	2.0405	Compressive Strength [37]	20°
2	AC-C2	-	100	100	100	2.0789	Compressive Strength [37]	20°
3	AC-C3	-	100	100	100	2.1594	Compressive Strength [37]	20°
4	AC-M1	-	100	-	800	2.101	Marshall Stability Test [36]	60°
5	AC-M2	-	100	-	800	2.101	Marshall Stability Test [36]	60°
6	AC-M3	-	100	-	800	2.101	Marshall Stability Test [36]	60°
7	AC-C4	-	100	100	100	2.101	Compressive Strength [37]	20°
8	AC-C5	-	100	100	100	2.102	Compressive Strength [37]	60°
9	AC-C6	-	100	100	100	2.110	Compressive Strength [37]	2°
10	ACC-C1	Copper	100	100	100	2.075	Compressive Strength [37]	20°
11	ACC-C2	Copper	100	100	100	2.075	Compressive Strength [37]	60°
12	ACC-C3	Copper	100	100	100	2.075	Compressive Strength [37]	2°
13	ACP-C1	PVC	100	100	100	2.063	Compressive Strength [37]	20°
14	ACP-C2	PVC	100	100	100	2.065	Compressive Strength [37]	60°
15	ACP-C3	PVC	100	100	100	2.067	Compressive Strength [37]	2°
16	AC-M4	-	100	-	800	2.095	Marshall Stability Test [36]	60°
17	AC-M5	-	100	-	800	2.101	Marshall Stability Test [36]	60°
18	AC-M6	-	100	-	800	2.085	Marshall Stability Test [36]	60°
19	ACC-M1	Copper	100	-	800	2.101	Marshall Stability Test [36]	60°
20	ACC-M2	Copper	100	-	800	2.095	Marshall Stability Test [36]	60°
21	ACC-M3	Copper	100	-	800	2.110	Marshall Stability Test [36]	60°
22	ACP-M1	PVC	100	-	800	2.077	Marshall Stability Test [36]	60°
23	ACP-M2	PVC	100	-	800	2.076	Marshall Stability Test [36]	60°
24	ACP-M3	PVC	100	-	800	2.081	Marshall Stability Test [36]	60°
25	AC-F1	-	100	500	100	2.095	Flexure Strength [38]	20°
26	AC-F2	-	100	500	100	2.101	Flexure Strength [38]	60°
27	AC-F3	-	100	500	100	2.085	Flexure Strength [38]	2°
28	ACC-F1	Copper	100	500	100	2.075	Flexure Strength [38]	20°
29	ACC-F2	Copper	100	500	100	2.075	Flexure Strength [38]	60°
30	ACC-F3	Copper	100	500	100	2.075	Flexure Strength [38]	2°
31	ACP-F1	PVC	100	500	100	2.066	Flexure Strength [38]	20°
32	ACP-F2	PVC	100	500	100	2.082	Flexure Strength [38]	60°
33	ACP-F3	PVC	100	500	100	2.075	Flexure Strength [38]	2°

2.3. Experimental Procedure

Marshall stability test, compressive strength test, and three-point bending test were the three tests carried out to investigate the structural performance of conventional asphalt pavement under different thermal conditions and to assess the change in its structural performance due to integrating the geothermal pipes into the asphalt body.

The stability and flow of the asphalt specimens were determined based on the ASTM D6927 [36]. Before the test, the asphalt specimens were immersed in water for 20 to 40 min until they achieved the test temperature. Then, the specimens were placed in the Marshall tester, as shown in Figure 5a. Prior to the test start, the flow meter was adjusted to zero. According to the test standard, loading rate of 50 mm per minute was employed until the peak load was achieved. Results of maximum load and flow were recorded. The average time that passed throughout the test between taking the specimens out of the water bath and determining the maximum load did not exceed 30 s.

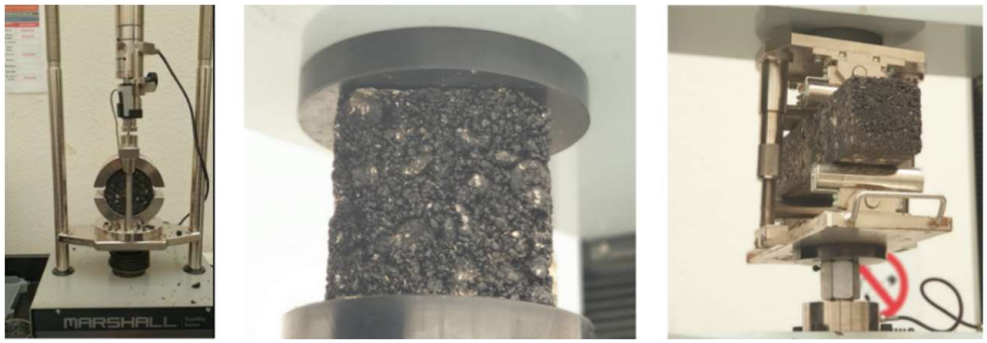

Figure 5. Laboratory tests included in the experimental study. (**a**) Marshall stability test. (**b**) Compressive strength test. (**c**) Flexure strength test.

The compressive strength of both conventional and geothermal asphalt specimens was examined according to the ASTM D1074 [37]. The test set-up is shown in Figure 5b; the top and bottom of the specimens were treated with Vaseline and a thin plastic sheet to minimize friction. Displacement transducers (LVDTs) were installed to measure the axial deformations of the specimens. The compressive strength of the specimens was calculated by dividing the maximum force (kN) of the UTM over the area (m^2) of the loaded surface.

The three-point bending test was conducted on 100 × 100 × 500 mm asphalt beams, as shown in Figure 5c. The test was performed based on a procedure developed by Judycki, 1990 [38]. A constant static load was applied to the AC beams for a time period ranging from 2400 s to 3600 s. The value of the applied load was dependent on the thermal condition, which means that it was variable depending on the temperature of the specimen. To ensure failure achievement, all specimens were subjected to a static load that led to exceeding 50% of the flexural strength. Typical test temperatures were 20 °C, 60 °C, and 2 °C to simulate the three thermal conditions, as explained before. The strain at the bottom of the specimen was measured with an LVDT sensor. As demonstrated in Figure 6, the test was carried out on three types of specimens: conventional asphalt specimens without geothermal pipes, asphalt specimens with 5/8′ PVC pipes, and AC specimens with 5/8′ copper pipes. In addition, the tests were performed on geothermal asphalt specimens in a steady-state situation, and no water circulation was applied.

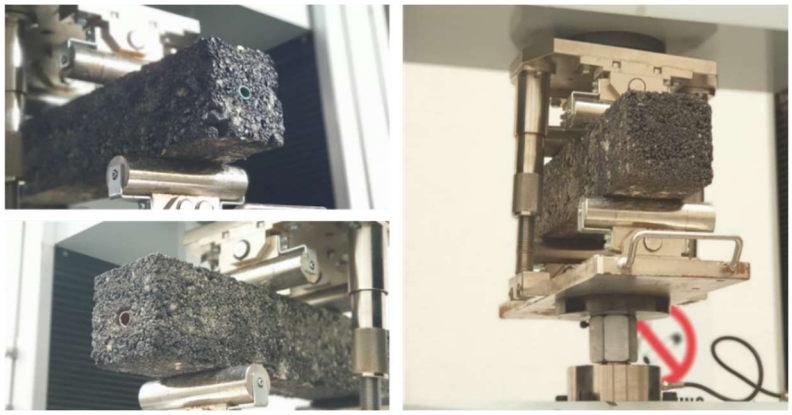

Figure 6. Three-point bending test conducted on asphalt specimens with and without geothermal pipes.

3. Results and Discussion

This section presents the results of the three laboratory tests performed within this experimental study. It also discusses the change in the asphalt structural performance under different thermal conditions that simulate extreme climate events. Furthermore, the change in the asphalt compressive and flexural strengths due to integrating two types of geothermal pipes is also explored.

3.1. Consistency of the Asphalt Specimens

Before digging into the comparative analyses, it was fundamental to ensure the consistency of the asphalt material among the whole specimens to avoid any discrepancies in results due to differences in specimen densities or compaction rates. Therefore, three specimens (AC-C_1, C_2, and C_3) were prepared, compacted at different rates, and tested in the compression test to explore the optimum density that should be maintained in the experimental study. Figure 7 presents the load–displacement results of the asphalt specimens upon the change in asphalt density.

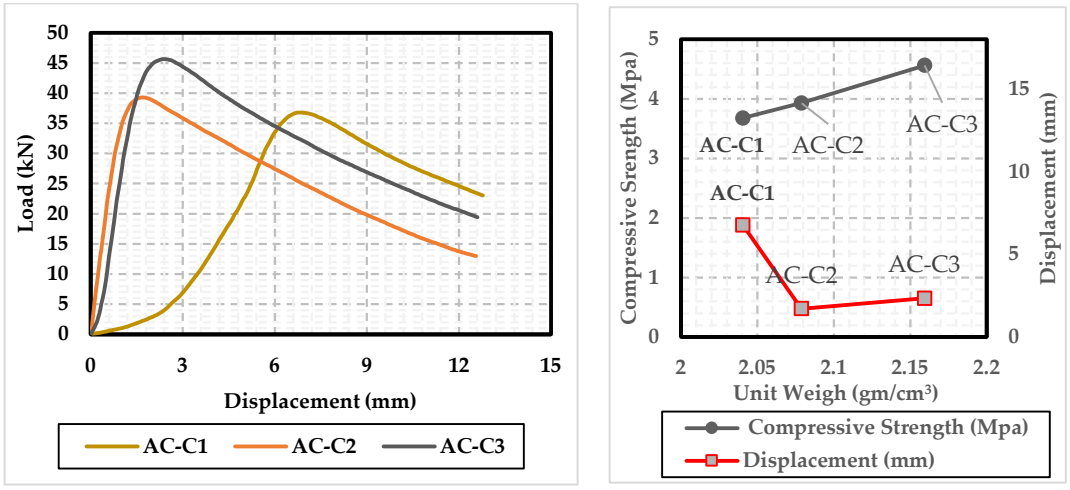

(**a**) (**b**)

Figure 7. (**a**) Compression test results of three AC specimens with different densities. (**b**) Relation between the AC density, the compressive strength, and displacement (20 °C).

It can be seen from Figure 7b that the AC compressive strength was linearly increasing with the AC density increases. Conversely, the displacement of the specimens decreased with the density increases. However, the change in load–displacement behavior became minimal after the AC density increased from 2.07 gm/cm^3 to 2.15 gm/cm^3. Therefore, the

density of 2.1 gm/cm^3 was adopted to unify the compaction effect while preparing the whole AC specimens included in the experimental study.

3.2. Structural Performance of Conventional Asphalt under Different Thermal Conditions

Three thermal conditions were applied to explore the change in the compressive and flexure strength of three identical specimens of conventional asphalt. Figure 8 highlights the compression load–displacement relationship change upon the asphalt temperature change.

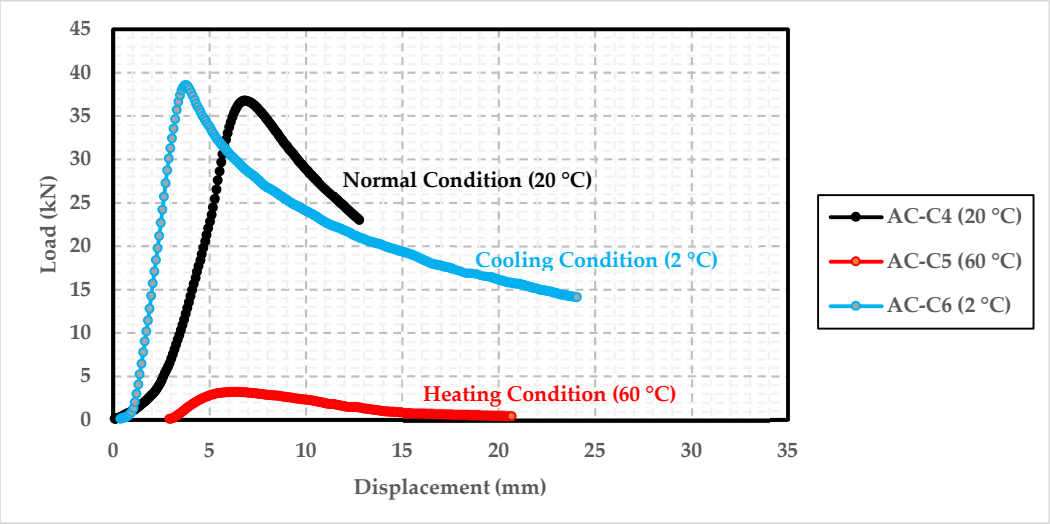

Figure 8. Asphalt compression load–displacement relationship under three thermal conditions.

At room temperature (20 °C), the max compression load and displacement achieved were 35.7 kN and 7.20 mm, respectively. With that in mind, the max compression load slightly increased (5.6%) under the cooling condition (2 °C), and the associated displacement decreased by 51.6%. In contrast, the maximum compression load dramatically dropped and decreased by 91.2% upon heating the specimen to 60 °C. As shown in Figure 8, the compression load–displacement became more ductile, and the elongation and displacement of the specimen became significantly high.

On the other hand, similar to the compression test, three conventional AC specimens were tested in a three-point bending test under three different thermal conditions. As pinpointed in Figure 9, although the flexure strength increased upon the cooling of the specimen, the failure became a brittle failure, not a ductile failure such as the AC at the normal temperature. Furthermore, the heating also had the same distractive effect on the asphalt.

The compressive and flexure strength test results prove that asphalt is a temperature-sensitive material; its mechanical properties and structural performance are firmly dependent on temperature variations. The results show that high temperature conditions had a distractive effect on the asphalt specimens; their compressive and flexure strengths dramatically decreased upon heating the specimens to 60 °C. This could be explained by the significant change in asphalt mixture viscosity. On the other hand, although the AC compressive and flexure strengths slightly increased upon cooling the specimen down to 2 °C, the AC behaved as a fragile solid, and its failure was described as brittle in that condition.

This may highlight the significant effect of climate change on asphalt pavements and explains the earlier deteriorations experienced nowadays in different countries. With that in mind, AC should be kept at medium temperatures, guaranteeing that it will maintain its viscoelastic structural behavior and preserve the deformation within safe limits. Shallow geothermal systems are capable of playing this significant role and contribute to the enhancement of asphalt pavements under extreme climates, as they are able to either cool

the pavement down during the hot climate or warm it up during the cold climate by exchanging the heat with the underlying subgrade layers.

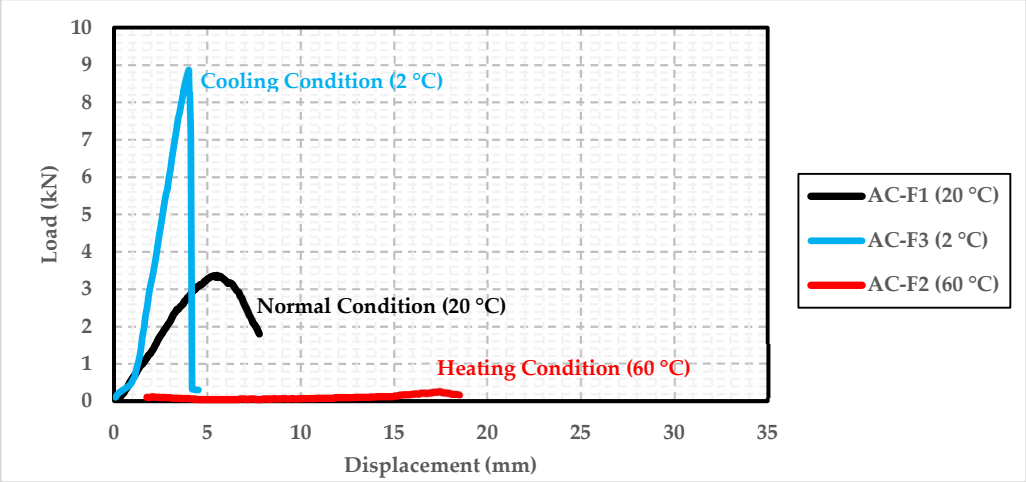

Figure 9. Asphalt flexure load–displacement relationship under three thermal conditions.

3.3. Effect of Geothermal Pipes on Asphalt Structural Behavior under Normal Thermal Conditions

The effect of two different pipe materials on the compressive strength, flexure strength, stability, and flow of the asphalt pavement was explored throughout a series of experimental tests at average normal room temperature (20 °C). The structural performance of the specimens equipped with the geothermal pipes was compared with the conventional ones to address the exact effects of the pipes on the behavior.

As shown in Figure 10, the compression load–displacement behavior of the conventional asphalt (AC-C) was compared with the ones with copper (ACC-C) and PVC pipes (ACP-C). It is fundamental to mention that both the copper and PVC pipes had the same diameter of 5/8′.

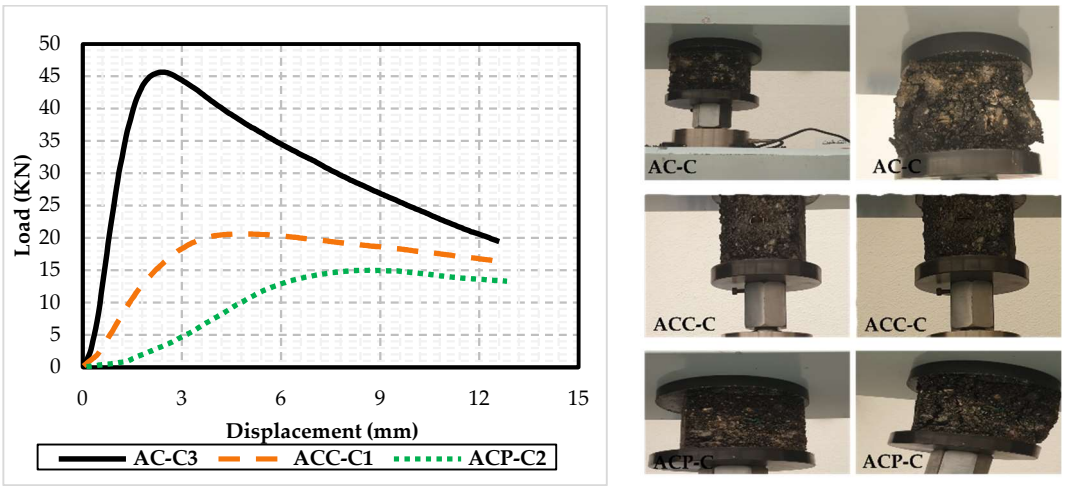

(**a**) (**b**)

Figure 10. (**a**) Effect of geothermal pipes on the asphalt compression strength (20 °C). (**b**) The failure mode of tested asphalt specimens with and without geothermal pipes.

Figure 10a indicated that the maximum compression load the AC specimen can sustain decreased by 55.4% and 66.67%, respectively, when the copper and PVC pipes were integrated into the asphalt body. The stiffness of the AC samples with the copper pipe was relatively higher than the ones with the PVC pipe.

The stability and flow behavior of the conventional AC specimens was compared with those with copper or PVC pipes throughout the Marshall tests. As demonstrated in Figure 11, the geothermal pipes had a relatively minimal effect on the stability of the AC specimens at normal average room temperature. However, the AC flow of the asphalt samples with copper and PVC pipes was 27.9% and 32.5%, respectively, and greater than the conventional AC.

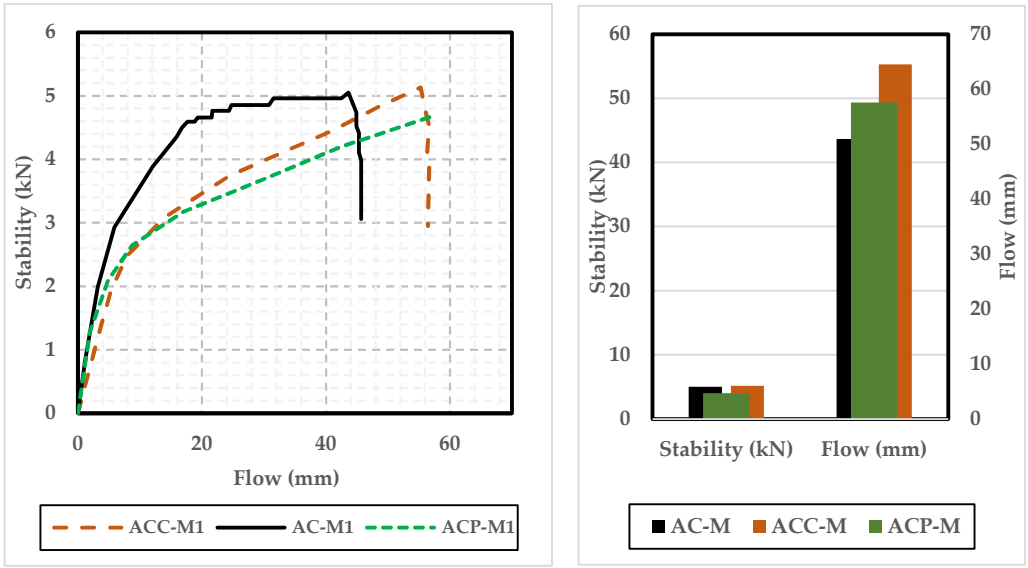

Figure 11. Effect of geothermal pipes on the asphalt Marshall stability. (**a**) Stability flow relationship. (**b**) Comparison between the results of three specimens.

On the other hand, a three-point bending test was performed to assess the change in AC flexural strength due to the integration of the copper and PVC geothermal pipes. As shown in Figure 12, the flexure capacity of the AC was significantly improved (14.3% increase percentage) by integrating the copper pipe. In contrast, the flexure strength of AC specimens dramatically decreased by 48.9% because of integrating the PVC pipes. It was also noted that the width of the induced flexure cracks at the failure state was less in the case of the AC samples with copper pipes (9 mm) compared to the ones with PVC or without pipes (24 mm).

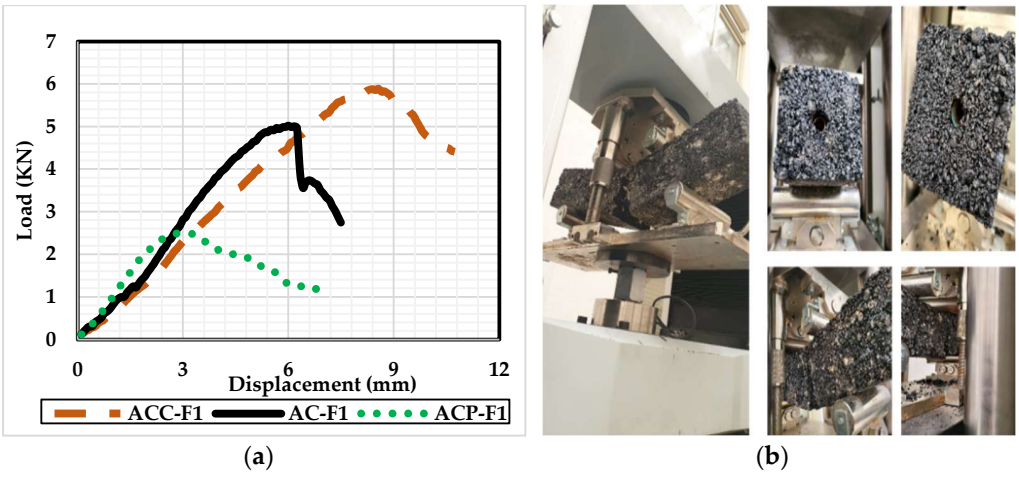

Figure 12. (**a**) Effect of geothermal pipes on the asphalt flexure strength (20 °C). (**b**) The failure of tested asphalt specimens with and without geothermal pipes.

The results of the three experimental tests carried out to assess the change in AC structural performance after integrating two types of geothermal pipes show that at a normal average temperature, the loss in AC volume due to geothermal pipe integration negatively affected the compressive strength of the asphalt. Nevertheless, it had an insignificant effect on the AC stability. In addition, selecting the appropriate geothermal pipe material can lead to a significant enhancement in flexural strength.

The presence of a pipe in the asphalt body resulted in a complex distribution of compression stresses and strains with peak stresses around the pipe. In addition, the existence of the pipes caused a change in the specimen failure mode. During the compression tests, it was noticed that for the AC with either copper or PVC pipes, parts of the asphalt material were being pushed out to the sides (Figure 10b), and the pipes were flattened. In addition, the asphalt material above the pipe was intact, indicating that the pipe was deformed, and the material next to the pipes took the load and failed.

In contrast, the integration of copper geothermal pipes into the asphalt body has significantly enhanced the flexural strength of the asphalt. However, this was not the case when the PVC pipe was utilized. This could be attributed to the high tensile and yield strengths of the copper material and the relatively low ultimate tensile strength and modulus of elasticity in the tension of the polyvinyl chloride material. On the other hand, regardless of the geothermal pipe type, a slippage between the AC and the geothermal pipe was observed at the failure of the specimens (see Figure 12b). This could be explained by the low bonding stress between the asphalt body and the surface areas of the pipes.

It is noteworthy to mention that at average room temperature, the geothermal pavement equipped with copper pipes revealed significantly superior structural performance compared to the one equipped with PVC pipes. This may be attributed to the difference in the modulus of elasticity and tensile strength of the copper compared to PVC.

3.4. Structural Performance of the Geothermal Pavement under Different Thermal Conditions

This section explores the change in both conventional and geothermal pavement behavior under heating and cooling conditions. The AC specimens with copper and PVC pipes were tested in terms of compression and flexure under different heating and cooling conditions. The embedded pipes were filled with water, and their ends were enclosed with impermeable filters, as shown in Figure 13b. The tested geothermal asphalt specimens under heating conditions were heated up to 60 °C, while others were cooled down to 2 °C. The results of the geothermal AC specimens were compared to the conventional AC ones under the same heating and cooling conditions.

Figure 13 compares the compression strength test results of both conventional and geothermal asphalt specimens under heating and cooling conditions. The compressive strengths of the geothermal asphalt with copper and PVC pipes were, respectively, 13.1% and 18.4% less than the conventional one under the heating condition. This result may indicate that the integration of geothermal pipes into the asphalt will not have a significant effect on the compression strength of AC in extreme climate events.

Similarly, the flexure strength test was carried out to assess the behavior of geothermal asphalt under different thermal conditions. Figure 14 compares the flexural load displacement of conventional AC and the asphalt specimens equipped with copper and PVC pipes. The test results pinpoint that integrating the copper pipes into the asphalt has enhanced the flexural performance of the asphalt under both heating and cooling conditions. The flexure strength of the geothermal asphalt with copper pipes was 85% and 70% greater than the conventional asphalt under the cooling and heating conditions, respectively. In contrast, integrating the PVC pipes into the specimens resulted in a minimal effect on the flexural strength of the AC specimens.

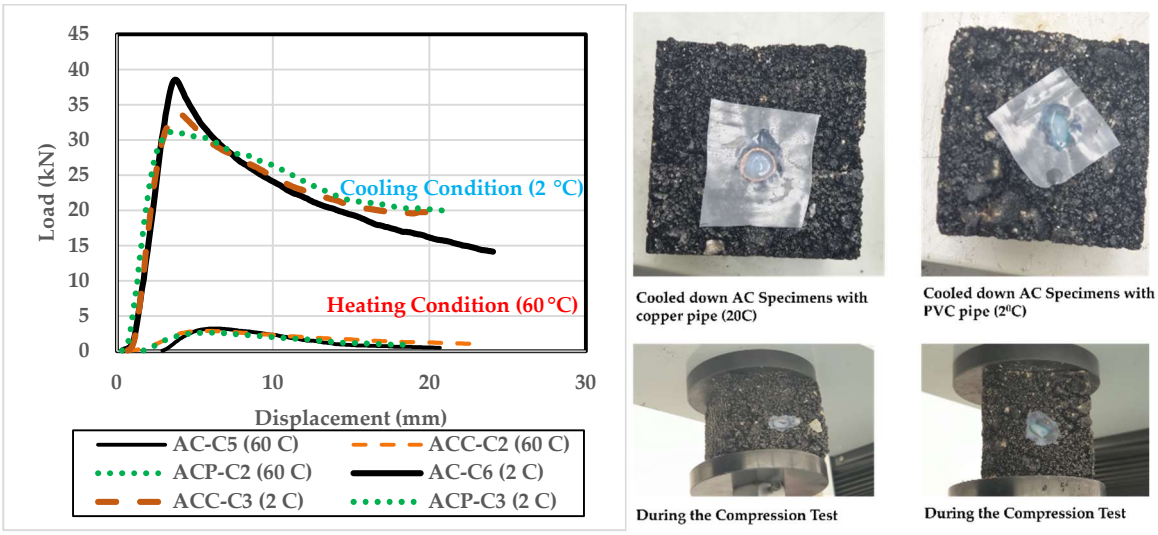

Figure 13. (**a**) Effect of geothermal pipes on the asphalt compression strength at heating (60 °C) and cooling (2 °C) conditions. (**b**) Comprehensive strength tests of the geothermal asphalt specimens.

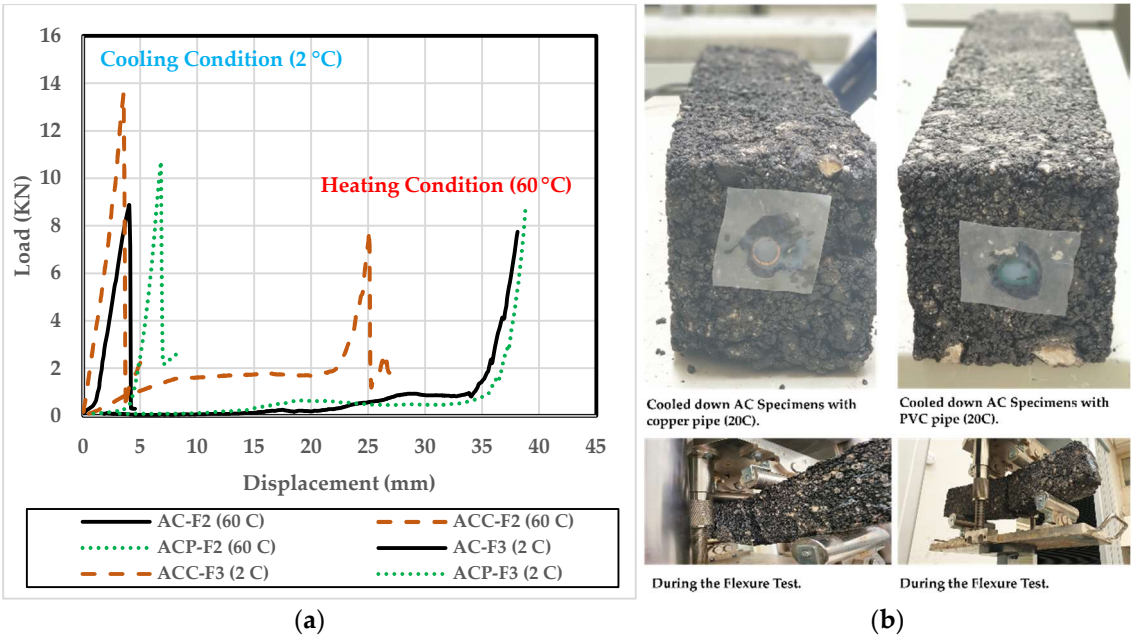

Figure 14. (**a**) Effect of geothermal pipes on the asphalt flexure strength at heating (60 °C) and cooling (2 °C) conditions. (**b**) Flexure strength tests of the geothermal asphalt specimens.

The results of compression and three-point bending tests under the heating and cooling conditions reveal that the behavior of the geothermal asphalt was consistent with conventional asphalt under extreme climate events. Brittle failure was observed in the geothermal AC specimens under cooling conditions, while a significant ductile failure was noticed under the heating condition. However, both the copper and the PVC pipes contributed to decreasing the induced cracks at the flexural failure, and the average width of the generated cracks at the failure was 80% and 70% less than the conventional specimens for the AC without copper and PVC, respectively. This could be explained by the ultimate tensile strength and relatively high modulus of elasticity of the geothermal pipes; these properties may empower the pipes to act as a reinforcement and strengthen the asphalt beams against flexural deformations.

Compared to the results of normal room temperature tests (See Figure 10), the drop in compression load displacement of the specimens with geothermal pipes was minimal under the heating and cooling conditions. This may shed light on how the geothermal systems may positively contribute to eliminating the associated asphalt pavement distresses in extreme climate events.

4. Conclusions

This paper discussed the structural behavior of conventional asphalt (AC) pavements under normal and extreme heating or cooling conditions. It has also introduced geothermal systems as a potential solution to eliminate the expected asphalt deterioration due to the recently experienced climate change events. Throughout the conducted experimental study, the change in the asphalt pavement structural performance due to the integration of geothermal pipes was assessed, and the following points were drawn:

- Asphalt is temperature-sensitive material; its mechanical properties and structural performance are firmly dependent on temperature variations.
- The compressive and flexure strengths of the conventional AC specimens dramatically decreased by about 92% upon heating the specimens to 60 °C. On the other hand, although the AC strengths slightly increased upon cooling down to 2 °C, the AC behaved as a fragile solid, and its failure was described as brittle.
- The results of this experimental study show that at a normal average temperature, the loss in AC volume due to the geothermal pipes integration negatively affected the compressive strength of the asphalt. However, under extreme heating and cooling conditions, geothermal pipes had a relatively minimal effect on the compressive strength of the asphalt specimens.
- The geothermal pipes had an insignificant effect on the stability of the AC specimens. However, the AC flow of the asphalt samples with copper and PVC pipes was 27.9% and 32.5% greater than the conventional AC.
- Under the three thermal conditions (medium, heating, and cooling temperatures), the flexure strength of the AC significantly improved by 14.3%, 85%, and 70%, respectively, due to the integration of the copper pipe into the asphalt body.
- The results of the experimental study show that copper pipes are superior to PVC ones in terms of enhancing the structural performance of AC under extreme hot and cold conditions.
- Asphalt pavements should be kept at medium temperatures, guaranteeing that the AC will maintain its viscoelastic structural behavior and preserve the deformation within safe limits. Shallow geothermal systems are capable of playing this significant role and contribute to the enhancement of asphalt pavement structural performance under extreme climates.

5. Limitations and Future Studies

- The tests presented in this experimental study were carried out in a steady-state situation, meaning that no water circulation was applied inside the pipes during the tests; in addition, static loading was utilized in the tests. Future research can be extended experimentally to explore the change in AC structural behavior during the transition from one thermal condition to another, i.e., from heating to medium temperature and to apply more tests, including dynamic loading. This might be beneficial in highlighting the influence of the geothermal system in maintaining the viscoelastic behavior of asphalt material.
- Including triaxial geogrid elements around the geothermal pipes could be used to overcome the stress concentration problem around the pipe and enhance the structural performance of the geothermal pipes.
- Increasing the bond stress between the asphalt medium and the geothermal pipe might also be an interesting area for improvement in terms of geothermal pavement structural performance. This could be achieved by using customized deformed copper

pipes with notches which are able to increase the contact surface area and the bond stress between the AC and the pipe.

Author Contributions: Conceptualization, M.E.A.-A., T.A.S. and Y.E.I.; methodology, M.E.A.-A. and T.A.S.; experimental testing, M.E.A.-A., A.M., M.A. and M.M.; validation, M.E.A.-A., Y.E.I. and A.M.; formal analysis, M.E.A.-A. and A.M.; investigation, M.E.A.-A. and T.A.S.; data curation, M.E.A.-A. and T.A.S.; writing—original draft preparation, M.E.A.-A.; writing—review and editing, M.E.A.-A., Y.E.I. and T.A.S.; visualization, M.E.A.-A.; supervision, M.E.A.-A. and Y.E.I. All authors have read and agreed to the published version of the manuscript.

Funding: This research was partly funded by the Prince Sultan University with a grant number of PSU-CE-SEED-74, 2021. In addition, it is supported by the Structures and Material (S&M) Research Lab of the Prince Sultan University.

Institutional Review Board Statement: Not applicable.

Informed Consent Statement: Not applicable.

Data Availability Statement: Not applicable.

Conflicts of Interest: The authors declare that they have no known competing financial interests or personal relationships that could appear to influence the work reported in this paper.

References

1. What Is Climate Change? Climate Action, United Nations. 2022. Available online: https://www.un.org (accessed on 2 April 2022).
2. Climate change Report, National Centers for Environmental Information, National Oceanic and Atmospheric Administration. 2020. Available online: https://www.ncdc.noaa.gov/sotc/global/202003 (accessed on 11 April 2022).
3. Newburger, E. As Earth Overheats, Asphalt Is Releasing Harmful Air Pollutants in Cities, CNBC. 2020. Available online: https://www.cnbc.com (accessed on 11 April 2022).
4. Al-Atroush, M.E.; Mustaffa, Z.; Sebeay, T.A. Emerging Trends in Overcoming the Weather Barrier to Sustainable Mobility in Gulf and Tropical Cities. ICSDI 2022. In *IOP Conference Series: Earth and Environmental Science*; IOP Publishing: Riyadh, Saudi Arabia, 2022; Volume 1026, p. 012040. [CrossRef]
5. Xie, J.; Zhou, Z. Numerical Analysis on the Optimization of Evaporative Cooling Performance for Permeable Pavements. *Sustainability* **2022**, *14*, 4915. [CrossRef]
6. Qiao, Y.; Dawson, A.R.; Parry, T.; Flintsch, G.; Wang, W. Flexible Pavements and Climate Change: A Comprehensive Review and Implications. *Sustainability* **2020**, *12*, 1057. [CrossRef]
7. Huang, Y.H. *Pavement Analysis and Design*; Prentice Hall Inc.: Upper Saddle River, NJ, USA, 1993; Volume 2.
8. Yinghao, M.; Jiajia, S.; Jin, Y. An Assessment of the Impact of Temperature Rise Due to Climate Change on Asphalt Pavement in China. *Sustainability* **2022**, *14*, 9044. [CrossRef]
9. Yoder, E.J.; Witczak, M.W. *Principles of Pavement Design*, 2nd ed.; JohnWiley & Sons, Inc.: Hoboken, NJ, USA, 1975. [CrossRef]
10. Underwood, B.S.; Guido, Z.; Gudipudi, P.; Feinberg, Y. Increased costs to US pavement infrastructure from future temperature rise. *Nat. Clim. Change* **2017**, *7*, 704–707. [CrossRef]
11. REPAIR PRIORITIES, Transportation for America, Taxpayers for Common Sense, Washington, DC. 2019. Available online: https://t4america.org/wp-content/uploads/2019/05/Repair-Priorities-2019.pdf (accessed on 11 April 2022).
12. Sun, L. Structural behavior of asphalt pavements: Intergrated analysis and design of conventional and heavy duty asphalt pavement. In *Butterworth-Heinemann, Chapter 2—Distribution of the Temperature Field in a Pavement Structure*; Elsevier: Oxford, UK, 2016; pp. 1–59. [CrossRef]
13. Emiliano, P.; Edoardo, B.; Maurizio, B. Effect of Bitumen Production Process and Mix Heating Temperature on the Rheological Properties of Hot Recycled Mix Asphalt. *Sustainability* **2022**, *14*, 9677. [CrossRef]
14. Dai, Z.; Shen, J.; Shi, P.; Zhu, H.; Li, X. Nano-sized morphology of asphalt components separated from weathered asphalt binders. *Constr. Build. Mater.* **2018**, *182*, 588–596. [CrossRef]
15. Menapace, I.; Yiming, W.; Masad, E. Chemical analysis of surface and bulk of asphalt binders aged with accelerated weathering tester and standard aging methods. *Fuel* **2017**, *202*, 366–379. [CrossRef]
16. Sun, X.; Yuan, J.; Zhang, Y.; Yin, Y.; Lv, J.; Jiang, S. Thermal aging behavior characteristics of asphalt binder modified by nano-stabilizer based on DSR and AFM. *Nanotechnol. Rev.* **2021**, *10*, 1157–1182. [CrossRef]
17. Sun, L. Structural behavior of asphalt pavements: Intergrated analysis and design of conventional and heavy duty asphalt pavement. In *Butterworth-Heinemann, Chapter 4—General Damage Characteristics for Asphalt Pavement*; Elsevier: Oxford, UK, 2016; pp. 243–295. [CrossRef]
18. Hans, S.; Nikola, J.; David, B. Development of a Calculation Concept for Mapping Specific Heat Extraction for Very Shallow Geothermal Systems. *Sustainability* **2022**, *14*, 4199. [CrossRef]

19. Riccardo, B.; Roberto, B.; Dario, F.; Giampaolo, M.; Maria, L.P.; Franco, S. Life Cycle Analysis of a Geothermal Power Plant: Comparison of the Environmental Performance with Other Renewable Energy Systems. *Sustainability* **2020**, *12*, 2786. [CrossRef]
20. Ho, I.-H.; Dickson, M. Numerical modeling of heat production using geothermal energy for a snow-melting system. *Geomech. Energy Environ.* **2017**, *10*, 42–51. [CrossRef]
21. Chiarelli, A.; Dawson, A.R.; García, A. Pavement temperature mitigation by the means of geothermally and solar heated air. *Geothermics* **2017**, *68*, 9–19. [CrossRef]
22. Cristina, S.B.; David, B.-D.; Ignacio, M.N.; Miguel, Á.M.; Arturo, F.M.; Diego, G.-A. Geothermal Heat Pumps for Slurry Cooling and Farm Heating: Impact and Carbon Footprint Reduction in Pig Farms. *Sustainability* **2022**, *14*, 5792. [CrossRef]
23. Kovačević, M.S.; Bačić, M.; Arapov, I. Possibilities of underground engineering for the use of shallow geothermal energy. *Građevinar* **2013**, *64*, 1019–1028. [CrossRef]
24. Al-Qadami, E.H.H.; Mustaffa, Z.; Al-Atroush, M.E. Evaluation of the Pavement Geothermal Energy Harvesting Technologies towards Sustainability and Renewable Energy. *Energies* **2022**, *15*, 1201. [CrossRef]
25. Fisher, D.E.; Rees, S.J.; Padhmanabhan, S.K.; Murugappan, A. Implementation and validation of ground-source heat pump system models in an integrated building and system simulation environment. *HVAC R Res.* **2006**, *12*, 693–710. [CrossRef]
26. Kakaç, S.; Yener, Y. *Heat Conduction*, 4th ed.; Taylor and Francis Group: Boca Raton, FL, USA, 2008.
27. Cullin, J.R.; Spitle, J.D.; Montagud, C.; Ruiz-Calvo, F.; Rees, S.J.; Naicker, S.S.N.; Konečný, P.; Southard, L.E. Validation of vertical ground heat exchanger design methodologies. *Sci. Technol. Built Environ.* **2015**, *21*, 137–149. [CrossRef]
28. Zeng, H.Y.; Diao, N.R.; Fang, Z. A finite line-source model for boreholes in geothermal heat exchangers. *Heat Transfer—Asian Res.* **2002**, *31*, 558–567. [CrossRef]
29. Bobes-Jesus, V.; Pascual-Muñoz, P.; Castro-Fresno, D.; Rodriguez-Hernandez, J. Asphalt solar collectors: A literature review. *Appl. Energy* **2013**, *102*, 962–970. [CrossRef]
30. Ministry of Municipal and Rural Affairs and Housing. Laws, Regulations and the Like. 2022. Available online: https://momrah.gov.sa/ar/regulations?pageNumber=2&type=224 (accessed on 28 June 2022).
31. ASTM D6913-04. Standard Test Methods for Particle-Size Distribution (Gradation) of Soils Using Sieve Analysis. ASTM International, USA. Available online: https://www.astm.org/d6913-04r09.html (accessed on 11 April 2022).
32. AASHTO, M. *Standard Specification for Performance-Graded Asphalt Binder*; American Association of State Highway and Transportation Officials: Washington, DC, USA, 2017.
33. ASTM B280-20. Standard Specification for Seamless Copper Tube for Air Conditioning and Refrigeration Field Service. ASTM International, USA. Available online: https://www.astm.org/b0280-20.html (accessed on 11 April 2022).
34. Copper, Copper Development Association Inc. Available online: https://alloys.copper.org/alloy/C10200 (accessed on 2 October 2022).
35. PVC Properties, Polyvinyl Chloride (PVC), Vinidex by Aliaxis. Available online: https://www.vinidex.com.au/technical-resources/material-properties/pvc-properties/ (accessed on 2 October 2022).
36. ASTM D6927-05. Standard Test Method for Marshall Stability and Flow of Bituminous Mixtures. ASTM International, USA. Available online: https://www.astm.org/d6927-05.html (accessed on 11 April 2022).
37. ASTM D1074-17. Standard Test Method for Compressive Strength of Asphalt Mixtures. ASTM International, USA. Available online: https://www.astm.org/d1074-17.html (accessed on 21 April 2022).
38. Judycki, J. Bending Test of Asphaltic Mixtures under Statical Loading. In Design and Quality Control of Bituminous Mixes, Proceedings of the 4th International Symposium on the Role of Mechanical Tests for the Characterization, Budapest, Hungary, 23–25 October 1990; Book Series: RILEM Proceedings. Taylor & Francis: Oxfordshire, UK, 1990; Volume 8, pp. 207–227.
39. Olumide, M.O. Marshall stability and flow of lime-modified asphalt concrete. *Transp. Res. Procedia* **2016**, *14*, 685–693. [CrossRef]
40. Van Bijsterveld, W.T.; De Bondt, A.H. Structural aspects of asphalt pavement heating and cooling systems. In Proceedings of the Third International Symposium On 3d Finite Element Modeling, Design & Research, Amsterdam, The Netherlands, 2–5 April 2002.